Environ. Sci. Technol. **1998**, *32,* 2450−2460

Modeling the Production of and Competition for Hydrogen in a Dechlorinating Culture

DONNA E. FENNELL AND JAMES M. GOSSETT*

School of Civil and Environmental Engineering, 223 Hollister Hall, Cornell University, Ithaca, New York 14853

A comprehensive biokinetic model employing Michaelis−Menten-type kinetics, H_2 thresholds, and thermodynamic limitations on donor fermentation was used to describe both fermentation of electron donors and competition for the evolved H_2 between hydrogenotrophic tetrachloroethene dechlorinators and methanogens. Model simulations compared favorably to experimental data where delivery of H_2 to a tetrachloroethene dechlorinator was accomplished using the donors butyric acid, ethanol, lactic acid, and propionic acid. Fermentations of the different donors were characterized by different dynamic patterns of H_2 generation that were captured successfully by the model. Experimental data and model simulations show that the ability to use H_2 at appreciable rates at low levels provides a competitive advantage to dechlorinators over methanogens. Slowly fermented substrates producing lower H_2 levels—kinetically accessible to dechlorinators, but too low for significant use by methanogenic competitors—were more effective and persistent "selective" stimulators of dechlorination than rapidly fermented substrates producing higher H_2 levels—accessible to both dechlorinators and methanogens. Model simulations suggest that adding excessive levels of rapidly fermented, high H_2-level-generating donors in an attempt to overcome competition, instead results in a dominant methanogen population and an eventual failure of dechlorination. When stimulating dechlorination, the quality of the donor as well as the quantity added must be considered.

Introduction

Many of the recently identified tetrachloroethene (PCE) dechlorinators have been reported to use molecular hydrogen (H_2) as an electron donor (*1*−*4*), and of these, some *only* use H_2 (*3, 4*). H_2 is therefore an important electron donor to consider for in situ stimulation of reductive dechlorination of PCE. H_2 is produced by fermentative organisms, and in natural environments, it is consumed by (among others) methanogens, sulfate-reducing bacteria, and ferric iron-reducing bacteria. Investigators have used H_2 level as one of a number of parameters to characterize zones in contaminated plumes as methanogenic, sulfate reducing, or iron reducing (*5*). Each hydrogenotroph has a different threshold or minimum level of H_2 at which it can operate. Under H_2-limiting conditions, H_2 is poised at a level that corresponds to the dominant microbial activity. At sites contaminated with chlorinated solvents, hydrogenotrophic dechlorinators must also compete for this limited donor.

Two recent reports suggest that dechlorinators possess a higher affinity for H_2 than do methanogens. Smatlak et al. (*6*) reported a 10-fold lower half-velocity coefficient (100 nM) for H_2 use by dechlorinators than for hydrogenotrophic methanogens (960 nM) in a mixed culture. Ballapragada et al. (*7*) reported half-velocity coefficients of 9−21 nM for H_2 use by dechlorination in a mixed culture. Thermodynamic considerations suggest that this high affinity for H_2 may be generally true of hydrogenotrophic dechlorinators. Since PCE dechlorination is energy yielding down to extremely low H_2 levels (*8*), it is likely that dechlorinators would have evolved with the ability to use H_2 at low, but still energetically favorable, concentrations.

Many different organic substrates become H_2 sources when fermented under anaerobic conditions (Table 1). However, the levels of H_2 resulting from their fermentation can differ by orders of magnitude, depending on the intrinsic thermodynamics of the particular fermentation reaction. We previously investigated four different organic H_2 sources—butyric acid, ethanol, lactic acid, and propionic acid—with widely different H_2-production ceilings (i.e., maximum levels of H_2 that could be thermodynamically achieved via fermentation). These studies demonstrated that substrates fermented only under low H_2 partial pressures (e.g., butyric and propionic acids) are superior donors for stimulating dechlorination while minimizing competing methanogenesis (*9*). If anaerobic reductive dechlorination is to become a widely used bioremediation technology, it is important that we understand and be able to model and predict the fate of applied donor and the extent to which it is channeled to desirable dechlorination or is wasted on stimulating the growth of competing organisms.

Many of the existing subsurface pollutant fate-and-transport models that are advocated for modeling dechlorinating systems were developed for predicting petroleum hydrocarbon transport and degradation. However, halogenated solvents serve as electron acceptors and are used only by a limited number of microorganisms with a restricted suite of electron donors—donors often in limited supply. In contrast, petroleum hydrocarbons serve as donors and the organisms that oxidize them are nearly ubiquitous; consequently, modeling dechlorination using petroleum-hydrocarbon-derived models is generally inappropriate. Furthermore, many of the available fate-and-transport models use half-life coefficients computed from historical data and first-order kinetics for predicting dechlorination. Such a simplistic approach is unwise because the presence, availability, and kinetics of the crucially important electron donors are not even considered, and it is unrealistic to assume that the same donor, redox, and microbial population conditions that were present in the past will continue into the indefinite future.

Wiedemeier et al. (*10*) provided an overview of some of the many analytical and numerical fate and transport models currently available for evaluating contaminant transport and degradation. Most were developed for fuel hydrocarbons. All but a few use first-order decay as the kinetic model for contaminant degradation (some also have zero- or multiple-order options). RT3D (*11*), which includes a kinetic package for reductive dechlorination, BIOPLUME III (*12*), and UTCHEM (*13*) incorporate more elaborate biodegradation schemes including Monod kinetics. One model includes both chloroethene and electron-donor degradation kinetics, equations for the conversion of an applied donor to endproducts thought to be used by dechlorinators, and competitive

* Corresponding author. Phone: (607) 255-4170; fax: (607) 255-9004; e-mail: jmg18@cornell.edu.

S0013-936X(98)00136-9 CCC: $15.00
Published on Web 07/03/1998

TABLE 1. Fermentation Reactions for Hydrogen Donors Examined during This Study (*25*)[a]

	$\Delta G_{35°C}$ (kJ/mol)
Fermentation to Acetate and H_2	
$butyrate^- + 2H_2O \rightarrow 2acetate^- + H^+ + 2H_2$	123.16
$ethanol + H_2O \rightarrow acetate^- + H^+ + 2H_2$	84.85
$lactate^- + 2H_2O \rightarrow acetate^- + HCO_3^- + H^+ + 2H_2$	71.01
$propionate^- + 3H_2O \rightarrow acetate^- + HCO_3^- + H^+ + 3H_2$	166.9
Fermentation to Propionate and Acetate	
$ethanol + {}^2/_3HCO_3^- \rightarrow {}^2/_3propionate^- + {}^1/_3acetate^- + {}^1/_3H^+ + H_2O$	−26.41
$lactate^- \rightarrow {}^1/_3acetate^- + {}^2/_3propionate^- + {}^1/_3HCO_3^- + {}^1/_3H^+$	−40.26

[a] All species as aqueous.

inhibition between PCE and trichloroethene (TCE) (*14*). None of these models, however, incorporates biokinetic expressions necessary to model closely coupled syntrophic associations of hydrogen-producing and hydrogen-using microorganisms, with all their attendant, competitive considerations. These expressions must be included for an accurate description of donor degradation and its resulting stimulation of either reductive dechlorination or competing processes.

In microbial applications apart from dechlorination, several models have been used to describe processes dependent upon syntrophic associations of hydrogenic fermenters and hydrogenotrophic methanogens and their finely regulated interactions involving interspecies H_2 transfer (*15*−*21*). These models incorporate mathematical expressions for limitation on the rate of donor degradation when product formation begins to thermodynamically limit the fermentation.

We now report the development of a comprehensive biokinetic model to provide a more highly developed description of the microbial interactions that occur in mixed microbial communities including dehalorespirers. The model developed during this study encompasses the kinetics of dechlorination, thermodynamically controlled donor fermentation, methanogenic use of H_2 and acetate, and the growth of all involved microbial populations. Such a complex description—currently lacking in fate-and-transport models that are used for analyzing bioremediation schemes and data from naturally attenuated sites—will enable more accurate modeling of reductive dechlorination stimulated by H_2.

Experimental Methods

The experimental data used here for comparison with the model and most of the experimental methods were reported previously (*9*). A methanol-enriched, PCE-dechlorinating culture that was operated at 35 °C was used as inoculum for the cultures that were developed in these studies. The data shown come from semicontinuously operated reactors (160 mL serum bottles with 100 mL culture volumes), which were enriched with PCE and an electron donor—either butyric acid, ethanol, lactic acid, or propionic acid. A vitamin solution and fermented yeast extract (FYE) were routinely added as nutritional supplements during long-term operation (*9*). The serum bottles were incubated at 35 °C with rotary-platform agitation. Data were obtained from long-term operation, as well as from time-intensive studies in which reactants, intermediates, and products were monitored after batch additions of PCE and an electron donor.

Particulate Organic Matter. Biomass content of cultures was estimated from particulate organic nitrogen (PON). A 100 mL volume of enrichment culture sample or a basal-medium blank was filtered through a SUPOR-200, 0.2 μm filter (Gelman Sciences). Total Kjeldahl nitrogen (TKN) analysis was performed on the prepared filters according to Standard Methods (method 421) (*22*). The biomass content of the culture (mg of VSS/L) was estimated using the difference between the TKN of the sample and the TKN of the blank and assuming a microbial cell composition of $C_5H_7O_2N$ (*23*).

Model Development

Model Implementation. The model was constructed and implemented in STELLA Research 4.02 (High Performance Systems), and it mimicked semicontinuous operation of 100 mL enrichment cultures in 160 mL serum bottles (*9*). Pulse inputs of donor, PCE, and FYE were simulated, as were wasting and purging events. Chloroethenes were modeled with an aqueous phase—on which the biokinetics were based—and a gaseous phase. Mass transfer between the aqueous and gaseous phases was incorporated in the model for the chloroethenes and ethene (ETH) using constants determined elsewhere (*6*, *24*). H_2 and CH_4 were assumed to be in phase equilibrium. [Modeling interphase transport of H_2, in particular, required an extremely small time step (dt), ca. 0.0005 h, to avoid numerical instabilities; given the extremely small dt values necessary to capture dynamics of gas/liquid exchange, we felt justified in making an equilibrium assumption. We validated this assumption by performing a few simulations that included a mass-transfer module for H_2.] A more complete model description appears elsewhere (*25*).

Kinetic Model for Donor Fermentation. The model describing the degradation of the H_2 donors used Michaelis−Menten kinetics, but with the inclusion of the thermodynamic influence of product (e.g., acetate and H_2) formation on the rate of fermentation.

$$\frac{dMt_{donor}}{dt} = \frac{-k_{donor}X_{donor}(S - S^*)}{K_{S(donor)} + S} \quad (1)$$

where Mt_{donor} is the total amount of donor in the bottle (μmol); k_{donor} is the maximum specific rate of donor degradation (μmol/mg of VSS h); X_{donor} is the donor-fermenting biomass in the bottle (mg of VSS); $K_{S(donor)}$ is the half-velocity coefficient for the donor (μmol/L); S is the donor concentration (μmol/L); S^* is the hypothetical donor concentration that, under the instantaneous culture conditions, would result in $\Delta G_{rxn} = \Delta G_{critical}$, given the concentrations of all the other reactants and products at that instant; and t is the time (h).

S^* is the "equilibrium" concentration of S, and it is related to $\Delta G_{critical}$—some marginally negative free energy that the organisms must have available to live and grow (*26*−*31*):

$$\Delta G_{critical} = \Delta G^\circ_{35°C} + RT \ln\left(\frac{[products]}{S^*[other\ reactants]}\right) \quad (2)$$

S is the actual substrate concentration at a particular time and is related to ΔG_{rxn}—the free energy available from the fermentation at that point in time:

$$\Delta G_{rxn} = \Delta G^\circ_{35°C} + RT \ln\left(\frac{[products]}{S[other\ reactants]}\right) \quad (3)$$

Subtracting and simplifying,

$$S - S^* = S\left[1 - \exp\left(\frac{\Delta G_{rxn} - \Delta G_{critical}}{RT}\right)\right] = S\Phi \quad (4)$$

where,

$$\Phi = 1 - \exp\left(\frac{\Delta G_{rxn} - \Delta G_{critical}}{RT}\right) \quad (5)$$

Note that $1 \geq \Phi \geq 0$. $\Phi = 1$ when $\Delta G_{rxn} << \Delta G_{critical}$ and there is no thermodynamic limitation on donor fermentation, and $\Phi = 0$ when $\Delta G_{rxn} \geq \Delta G_{critical}$.

$(S - S^*)$ in eq 1 is replaced by $S\Phi$ as per eq 4, with Φ calculated using eq 5, giving eq 6—the form used in the STELLA implementation of the model.

$$\frac{dMt_{donor}}{dt} = \frac{-k_{donor}X_{donor}S\Phi}{K_{S(donor)} + S} \quad (6)$$

For each time increment, the ΔG_{rxn} for the donor fermentation was calculated using the instantaneous aqueous-phase concentrations (Cw) of the pertinent compounds. $\Delta G_{critical}$ was −19 kJ/mol donor. This free energy value—in many cases the maximum observed while the fermentations were ongoing —was determined from analysis of the ΔG_{rxn} at each time step in actual time-intensive studies (*25*). This value is similar to $\Delta G_{critical}$ values reported for fermentations of butyrate, ethanol, and benzoate (*26*−*31*). From ΔG_{rxn} and $\Delta G_{critical}$, Φ was calculated—anew for each time step—via eq 5.

Φ is a measure of the distance of the reaction from thermodynamic equilibrium. If the fermentation is far from equilibrium (i.e., the donor concentration is high relative to the concentrations of the products of the reaction, H_2 and acetate), the driving force is high, Φ approaches 1, and the fermentation reaction is limited primarily by intrinsic kinetics. As the reaction approaches equilibrium (i.e., donor concentration has decreased and H_2 and acetate have increased), the driving force is lessened, the value of Φ approaches zero, and the fermentation is limited primarily by thermodynamics. The model does not incorporate reversibility, but is otherwise similar in form to models which do (*17*−*21*). It was determined that substituting $(S - S^*)$ for S in the denominator of eq 1 had little impact on the fit of the model (data not shown).

The fermentation reactions included in the model and their respective $\Delta G^\circ_{35°C}$ values (the standard free energy of reaction at 35 °C, with all solutes at unit activity, and H_2 as an aqueous component) are shown in Table 1. Computation of the $\Delta G^\circ_{35°C}$ values is detailed elsewhere (*25*). The maximum specific rates of donor use, k_{donor}, and the half-velocity coefficients for donor use, $K_{S(donor)}$, estimated from nonlinear regression analysis of the donor degradation data that were collected during this study (*25*), are shown in Table 2. Note that these kinetic values are pertinent to the particular laboratory cultures and conditions (e.g., 35 °C) employed in our studies and are not prescribed for general use.

Kinetic Model for Dechlorination. Kinetics of dechlorination were of Michaelis−Menten form wherein the rate of dechlorination was described not only by the chloroethene concentration, but also by the H_2 concentration. Separate modules were incorporated for each of the chloroethenes, although TCE and dichloroethenes (DCEs) were not frequently detected species. With the use of the rate constants shown in Table 2, they were modeled to be degraded about as rapidly as they were produced. The DCE isomer of primary interest was *cis*-1,2-DCE and the DCE module included only constants for *cis*-1,2-DCE. The equations used to describe dechlorination are exemplified by that for PCE:

TABLE 2. Kinetic Parameters (35 °C) Utilized in the Model

fermentation	$k_{(donor)}$[a] (μmol/mg of VSS h)	$K_{S(donor)}$[a] (μmol/L)
butyrate$^-$ → acetate$^-$ + H_2	4.9	34.3
ethanol → acetate$^-$ + H_2	21.9	17
lactate$^-$ → acetate$^-$ + H_2	8.6	2.5
propionate$^-$ → acetate$^-$ + H_2	2.2	11.3
ethanol → propionate$^-$ + acetate$^-$	21.9	17
lactate$^-$ → propionate$^-$ + acetate$^-$	8.6	2.5

dechlorination	$k_{(chloroethene)}$ (μmol/mg of VSS h)	$K_{S(chloroethene)}$ (μmol/L)[d]
PCE	1.8[b]	0.54
CE	3[c]	0.54
cis-1,2-DCE	3[c]	0.54
VC	3[d]	290
H_2		0.1

methanogenesis	k (μmol/mg of VSS h)	K_S (μmol/L)
H_2	40[e]	0.5[f]
acetate	5.65[g]	1000[g]

[a] Determined from data collected during time-intensive studies (*25*). [b] Reference *4*. [c] Estimated (*40*). [d] Reference *24*. [e] Estimate, this study and refs *41* and *24*. [f] Within range of reported values (*6*, *42*−*44*). [g] References *45* and *46*.

$$\left(\frac{dMw_{PCE}}{dt}\right)_{degradation} = \frac{-k_{PCE}X_{dechlor}Cw_{PCE}}{K_{S(PCE)} + Cw_{PCE}} \times \frac{(Cw_{H2} - H_2\ threshold_{dechlor})}{K_{S(H2)dechlor} + (Cw_{H2} - H_2\ threshold_{dechlor})} \quad (7)$$

where Mw_{PCE} is the total amount of PCE in the aqueous phase (μmol); k_{PCE} is the maximum specific rate of the PCE utilization (μmol/mg of VSS h); $X_{dechlor}$ is the dechlorinator biomass contained in the serum bottle (mg of VSS); Cw_{PCE} is the aqueous PCE concentration (μmol/L); $K_{S(PCE)}$ is the half-velocity coefficient for PCE use (μmol/L); Cw_{H2} is the aqueous H_2 concentration (μmol/L); $K_{S(H2)dechlor}$ is the half-velocity coefficient for H_2 use by dechlorinators (μmol/L); and H_2 $threshold_{dechlor}$ is the threshold for H_2 use by dechlorinators (μmol/L).

It was assumed that the same biomass, $X_{dechlor}$, was responsible for each step of the dechlorination. Since TCE and DCE did not appear as significant, persistent intermediates in these systems, competitive inhibition between the chloroethenes was not included in the model at this time. The parameters used in the kinetic model for chloroethene and H_2 use by dechlorinators were taken or estimated from previous studies (Table 2). The H_2 $threshold_{dechlor}$—the lowest H_2 level at which dechlorination was observed—was estimated from data collected during this study (data not shown) to be at least as low as 0.0015 μM.

Kinetic Model for Hydrogenotrophic Methanogenesis. Methanogenesis from H_2 was also modeled using a Michaelis−Menten-type kinetic equation which incorporated the threshold for H_2 use by methanogens:

$$\left(\frac{dMt_{CH4\ from\ H2}}{dt}\right)_{production} = \frac{1}{4}k_{(H2)meth}X_{hydrogenotroph} \times \frac{(Cw_{H2} - H_2\ threshold_{meth})}{K_{S(H2)meth} + (Cw_{H2} - H_2\ threshold_{meth})} \quad (8)$$

where $Mt_{CH4\ from\ H2}$ is the total CH_4 produced via hydrogenotrophs (μmol); $k_{(H2)meth}$ is the maximum rate of H_2 utilization (μmol/mg of VSS h); $X_{hydrogenotroph}$ is the hydrogenotrophic methanogenic biomass contained in the bottle (mg of VSS); Cw_{H2} is the aqueous hydrogen concentration

TABLE 3. Literature Yield Values for Bioprocesses Examined

bioprocess	*Y*	reference
	(mg of VSS/total μmol of substrate used)	
butyrate fermentation	0.002 79	*47*
ethanol fermentation (to acetate)	0.001 98	*39*
ethanol fermentation (to propionate)	0.002 97	*48*
lactate fermentation (to acetate)	0.003 51	*49*
lactate fermentation (to propionate)	0.005 63	*50*
propionate fermentation	0.001 44	*49*
acetotrophic methanogenesis	0.001 89	*51*
	(mg of VSS/μmol H_2 used for energy)	
dechlorination	0.006 12	*4*
hydrogenotrophic methanogenesis	0.001 43	*52*

(μmol/L); $K_{s(H2)meth}$ is the half-velocity coefficient for H_2 use by hydrogenotrophic methanogens (μmol/L); and H_2 Threshold$_{meth}$ is the threshold for H_2 use by hydrogenotrophic methanogens (μmol/L).

Kinetic parameters for H_2 use by methanogens are shown in Table 2. An H_2 Threshold$_{meth}$ of ca. 0.008 μM was estimated from experimental data by observing how high H_2 was before methanogenesis was observed (*9, 25*). The threshold value for methanogenesis from H_2 observed during this study is somewhat lower than some values (0.021−0.075 μM) cited in the literature for laboratory cultures (*32, 33*), but is within the range (0.005−0.02 μM) observed in predominantly methanogenic sediments and aquifers (*34, 35*).

Kinetic Model for Acetotrophic Methanogenesis. Acetotrophic methanogenesis was modeled using straightforward Michaelis−Menten kinetics and the kinetic parameters shown in Table 2.

Kinetic Model for Biomass Growth. Biomass growth was modeled separately for each distinct group of organisms in the mixed culture using eq 9.

$$\frac{dX}{dt} = Y\left(\frac{-dMt}{dt}\right) - k_d X \qquad (9)$$

where dMt/dt is the change in substrate of interest over the time increment (μmol/h); Y is the organism yield (mg of VSS/μmol substrate used); X is the biomass of the specific organism group contained in the bottle (mg of VSS); and k_d is the decay coefficient for the organism group (h^{-1}).

Yield values used for all aspects of the modeling are shown in Table 3. A decay rate, k_d, of 0.001 h^{-1} was assumed for all microbial groups. Note that vinyl chloride (VC) dechlorination to ETH by this dechlorinator is thought to be cometabolic (*4*), and thus, this step was assumed to yield no biomass growth.

Estimation of Biomass Fractions. While total biomass concentrations were measured for each enrichment culture, concentrations of individual populations—i.e., dechlorinators, fermenters, etc.—were not. The fractions of biomass made up by different organism groups were estimated using an analysis of steady-state influent and effluent concentrations of individual substrates and reported yields (Table 3). The initial biomass settings for each simulation are shown in Table 4. These analyses predicted total biomass concentrations that were very similar to those measured in the cultures (*25*), but the accuracies of the estimated distributions of total biomass among various microbial groups in the cultures are unknown.

Modeling Fermented Yeast Extract (FYE) Input. FYE contributed low levels of volatile fatty acids to the enrichment cultures and greatly influenced the outcome of long-term operation with the different donors (*9*). FYE added at feeding events was modeled as a trace pulse input of acetic, propionic, and butyric acids. The contributions were estimated from several analyses of the actual volatile fatty acid (VFA) content of FYE solutions and from determination of its reducing equivalent contribution (*9, 25*). Excess reducing equivalents that were not accounted for by the measured VFA content were simulated by increasing the proportion of butyric acid claimed to exist in FYE. For a 20 μL FYE addition, the following pulse inputs were added: acetic acid = 1.37 μmol; propionic acid = 0.32 μmol; and butyric acid = 3.87 μmol.

Modeling Endogenous Decay Contributions. Biomass decay contributes to the electron-donor pool. Since it is likely that initial products of organism decay are subject to the same thermodynamic limitations as the other donors, decay was modeled as a contribution to butyric acid—a slowly available "model" compound. Decay from each of the biomass pools was channeled on a 1:1 mol basis [based on biomass modeled as $C_5H_7O_2N$ and coupled half-reactions (*23*)] directly into the butyrate pool.

General Approach For Simulating Experimental Data. The biokinetic, thermodynamic, and physical/chemical parameters were entered in the model and remained fixed for all simulations shown here. The initial individual biomass concentrations, amount and type of donor fed, and amount of FYE added (if any) were entered as appropriate for the specific condition to be simulated. A specific simulation time was set, and the model was run using a model time step (dt) of 0.031 25 h and a Runge−Kutta 4 integration method. Simulations of time-intensive studies were run for a maximum of 48 h. Simulation of long-term operation runs were for about 100 days or until biomass, dechlorination products, and VFA content stabilized. Output was overlaid on experimental data to examine closeness of fit.

Results

Test of Model Using Steady-Condition Data from the Butyrate Source Culture. The model was first tested against data collected from a butyric-acid-enriched source culture which had been operated at a 2:1 (equiv/equiv) ratio of butyrate to PCE for 2.2 years (*9*). If the model were adequate to describe the culture, then initialization with an arbitrarily chosen biomass content and subsequent simulation at the routinely amended donor, FYE, and PCE levels should result in eventual stabilization at the experimentally observed steady-state biomass, methanogenesis, and dechlorination levels. A 108 day simulation did show culture stabilization at approximately the steady-state total biomass concentration and the same levels of PCE dechlorination and methanogenesis as observed in the laboratory culture (Table 5). The major difference between simulated and observed performances was in the extent of VC's conversion to ETH; the simulation predicted that less of the VC formed from PCE would be converted to ETH than was actually observed.

The final biomass distribution obtained from the long-term simulation was used as an input to model short-term, time-intensive performance data collected from this butyrate culture. Again, under these conditions, the model fit the data well (*25*).

Simulation of Time-Intensive Tests for H_2 Donors. The model was employed to simulate experimental results from short-term, time-intensive studies (TISs) of enrichments amended with either a 1:1 or 2:1 (equiv/equiv) donor to PCE ratio, with butyric acid, ethanol, lactic acid, or propionic acid as donor. The estimated biomass distribution was entered as a model input, and the donor amendment type and amount (μmol) and the PCE amendment (μmol) were adjusted to the same levels as those employed in experimental studies. FYE was omitted in modeled, as well as experimental, TISs. At the 2:1 donor:PCE ratio, complete results are presented only for butyric acid, ethanol, and propionic acid.

TABLE 4. Initial Biomass (mg of VSS/100 mL) Used for Time-Intensive Study Simulations

TIS	total	donor fermenter	butyric acid fermenter	propionic acid fermenter	acetotrophic methanogen	hydrogenotrophic methanogen	dechlorinator
butyric acid 1:1	3.68	0.77		0	0	0.12	2.70
butyric acid 2:1	6.99	1.51		0.004	1.71	0.84	2.93
ethanol 1:1	3.23	0.52	0.13	0.002	0	0.35	2.23
ethanol 2:1	3.54	0.62	0.15	0.0014	0.56	0.67	1.54
lactic acid 1:1[a]	3.51	0.53 (to HAc) 0.36 (to Prop)	0.12	0.052	0	0.14	2.31
lactic acid 2:1[a]	3.96	0.76 (to HAc) 0.52 (to Prop)	0.15	0.085	0.5	0.69	1.26
lactic acid 2:1	3.96	1.16	0.16	0.0008	0.54	0.74	1.36
propionic acid 1:1	2.27	0.14	0.074		0	0.01	2.05
propionic acid 2:1[b]	6.52	0.43	0.22		0.35	0.29	5.01

[a] Assumes that 30% of the lactate is fermented via the propionate fermentation pathway. [b] Model used an acetotroph population of 60% of that predicted since the culture was clearly not at steady state with respect to acetogenesis.

TABLE 5. Comparison of Values Obtained from a Source Culture and a Long-Term Model Simulation Fed a 2:1 (equiv/equiv) Ratio of Butyric Acid to PCE

parameter	culture, day 402−day 804	model, day 60−day 104
average ETH (μmol/feeding)	11	6.5
average VC (μmol/feeding)	1.1	4.5
average total methane (μmol/feeding)	126.3	113
average total reduction products (μequiv/feeding)	1105	983
ending total biomass (mg of VSS/L)	71.6	64.8

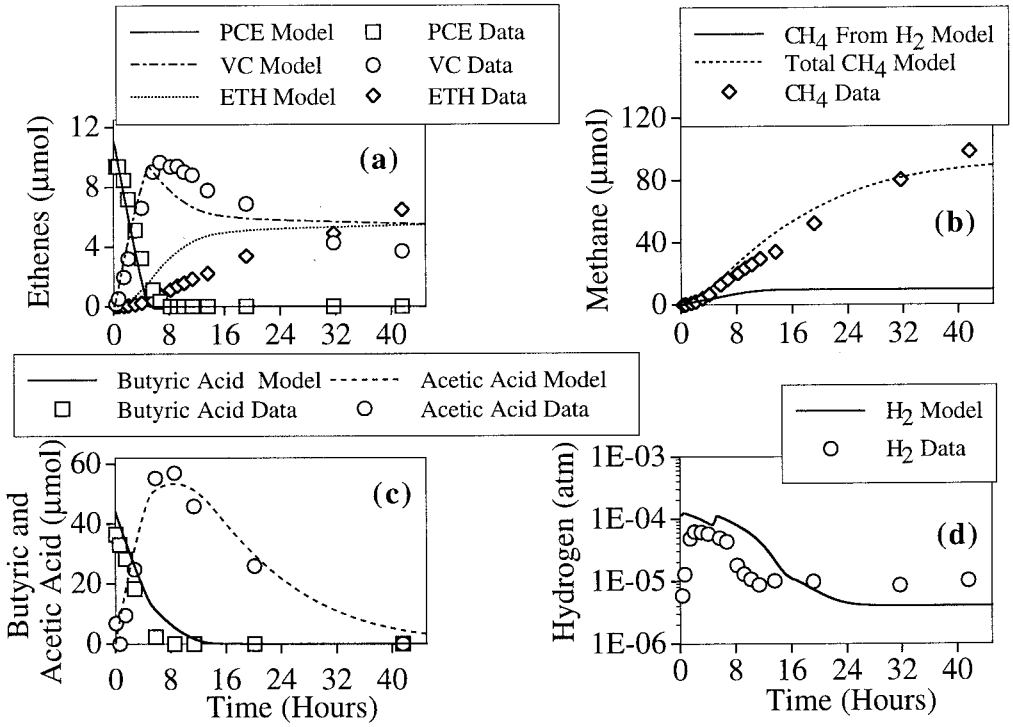

FIGURE 1. Comparison of butyric acid-amended culture fed 2:1 (equiv/equiv) donor to PCE ratio with model prediction: (a) dechlorination; (b) methane; (c) VFAs; and (d) hydrogen.

At the 1:1 ratio, complete results are shown only for ethanol. Simulated and observed H_2 patterns are presented for both administered ratios of all four donors.

(a) Butyric Acid 2:1 Ratio to PCE. Figure 1 depicts a 2:1 butyric acid-amended culture simulation overlaid with experimental data from a 2:1 TIS. The model predicted faster VC dechlorination to ETH than was observed experimentally (Figure 1a), then a gradual cessation as butyric acid and the resulting H_2 pool were depleted. Predictions of methanogenesis (Figure 1b), butyric acid degradation, acetic acid formation and depletion (Figure 1c), and the ultimate H_2 level generated (Figure 1d) were fairly close to those actually observed. Experimentally, VC dechlorination continued slowly after butyric acid was depleted and the level of H_2 persisting in the bottle was slightly higher than that predicted by the model—suggesting that some other source of donor was available that was not reflected in the model. No propionic acid was present and FYE was not added. One possibility is that the conversion of acetic acid to CH_4, which occurred until nearly the end of the test, supplied reducing equivalents (not accounted for in the model) that were being scavenged by the dechlorinators (*36, 37*).

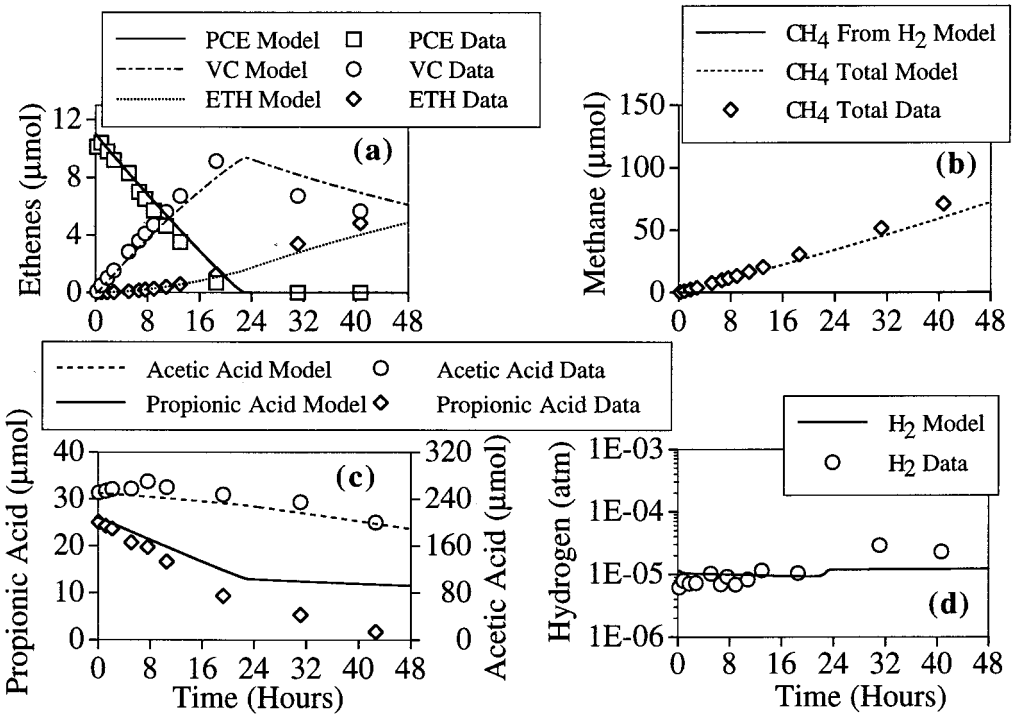

FIGURE 2. Comparison of propionic acid-amended culture fed 2:1 (equiv/equiv) donor to PCE ratio with model prediction: (a) dechlorination; (b) methane; (c) VFAs; and (d) hydrogen.

(b) Propionic Acid 2:1 Ratio to PCE. The model fit to a 2:1 propionic acid-amended culture captured the overall shapes and trends of the data set very well (Figure 2), except that experimentally, propionic acid fermentation (Figure 2c) was more rapid and complete than predicted by the model. The model predicted that when PCE dechlorination—the primary H_2 sink—was satisfied (Figure 2a), the H_2 level increased (Figure 2d). That increase affected the thermodynamic situation and caused propionic acid fermentation to slow dramatically in the model. H_2 was then predicted only to be used by VC dechlorination—none was predicted to go to methanogenesis at that H_2 level. Experimentally, propionic acid fermentation appeared to be less affected by the disappearance of PCE and the slight increase in H_2 level (though a break in fermentation rate is evident in Figure 2c). Since acetotrophic activity was present, no separate determination of CH_4 production via H_2 was made experimentally. H_2 generated from the remaining propionic acid—if channeled to methanogenesis—would have added approximately 10 μmol of CH_4 to the total amount produced in the model simulation and would still fit the actual data fairly well (Figure 2b). This may have been the fate of the remaining propionate.

(c) Ethanol 2:1 Ratio to PCE. The fit of the model to a TIS of ethanol at a 2:1 ratio is shown in Figure 3. The model simulation fit the data from this study well, except that ethanol disappearance (Figure 3c) was more rapid than the model predicted. Experimentally, VC dechlorination continued slowly after ethanol was depleted. Again, it is possible that the conversion of acetic acid to CH_4, which occurred until the end of the test, supplied reducing equivalents that were scavenged by the dechlorinators (*36, 37*).

(d) Ethanol 1:1 Ratio to PCE. A fit of the model to data from two replicate 1:1 ethanol-amended cultures is shown in Figure 4. While the model captured the overall dynamic behavior of the TIS quite well, dechlorination (Figure 4a) was predicted to occur more rapidly than was actually observed, less CH_4 was predicted than was actually formed (Figure 4b), and ethanol disappeared slightly more rapidly than observed (Figure 4c). The H_2 level was predicted well; however, the persistence of H_2 was longer in actuality than the model predicted (Figure 4d). With this example, it can be noted that when the ethanol was totally consumed, about 40% of the PCE remained.

(e) Summary of Results of Short-Term Time-Intensive Model Fits. The outcomes of the simulations may best be summarized by a comparison of actual H_2 data with the H_2 predicted by the model under each condition. Figure 5 presents results for both 1:1 and 2:1 administered ratios of all four donors. While discrepancies certainly are evident between simulated and observed H_2 levels, it is apparent that the model was able to capture the dynamics of H_2 production/consumption quite well—i.e., the substantive differences in dynamic H_2 patterns among the four donors.

Exploration of the Role of FYE in Sustaining Dechlorination during Long-Term Operation of Ethanol-Amended Cultures. Previous experimental results showed that the addition of FYE (and the trace amounts of VFAs that it contained) significantly influenced the extent of dechlorination during long-term culture operation (*9*). Even ethanol—a donor which in both actual and modeled TISs resulted in incomplete dechlorination and significant residual PCE—produced excellent dechlorination results over the long-term when FYE was coamended. Long-term operation without FYE was not tested during the experimental study since FYE was a required nutritional source and could not be omitted for long periods without the danger of introducing a nutritional deficiency. Using the developed model, which appeared to accurately capture the performance of these cultures, we explored the long-term role of FYE in a way that we could not, experimentally.

(a) Simulations of Ethanol at a 1:1 Ratio. Long-term simulations were run for ethanol at a 1:1 donor to PCE ratio both with and without FYE addition. Long-term simulations used the biomass inputs for ethanol at a 1:1 ratio shown in Table 4. The repetitive amendment amounts were 22 μmol of ethanol and 11 μmol of PCE. FYE, when added, was 20 μL. The experimentally observed background concentrations of acetic and propionic acids were also entered.

Figure 6 shows long-term simulation of 1:1 ethanol without FYE addition. Again, this condition was not exam-

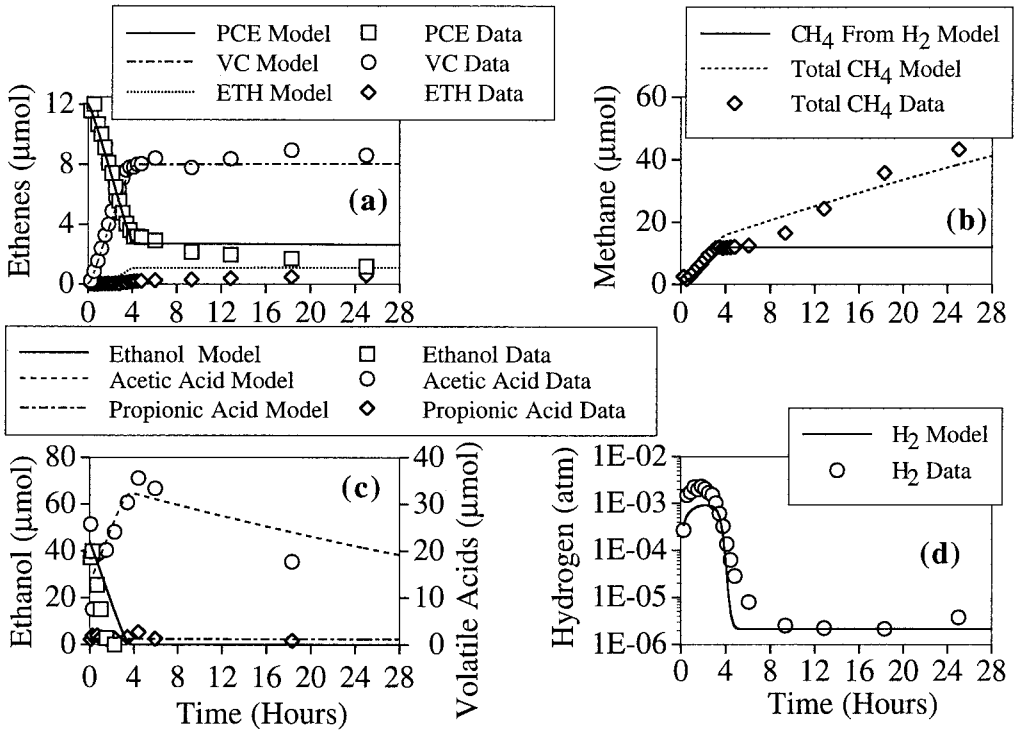

FIGURE 3. Comparison of ethanol-amended culture fed 2:1 (equiv/equiv) donor to PCE ratio with model prediction: (a) dechlorination; (b) methane; (c) ethanol and VFAs; and (d) hydrogen.

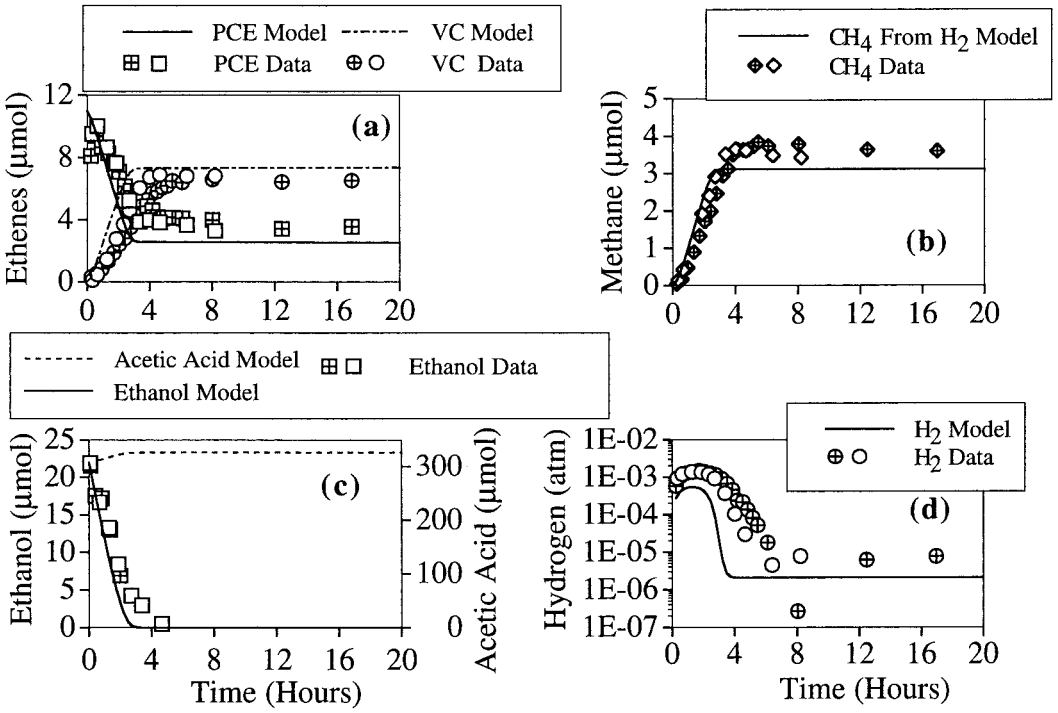

FIGURE 4. Comparison of ethanol-amended culture fed 1:1 (equiv/equiv) donor to PCE ratio with model prediction: (a) dechlorination; (b) methane; (c) ethanol and acetic acid; and (d) hydrogen.

ined experimentally, since without knowing the detailed micronutrient requirements of the dechlorinator, we thus far are unable to operate cultures long-term in the absence of FYE. PCE dechlorination was incomplete during this simulation, although it became slightly more complete over time (Figure 6a). The CH_4 production decreased during the simulation (Figure 6b). The sawtooth appearance of the graphs is a result of the repetitive addition of PCE and donor every second day. Since purging occurred only every fourth day, every other data point depicts the cumulative dechlorination product and methane formation resulting from two feedings. A trace amount of propionic acid, initially present to mimic the small amount that was found in actual ethanol-fed cultures, was slowly depleted from the system through biodegradation and washout, since there was no further input of propionic acid. Butyric acid accumulated slowly as a result of its generation through biomass decay (Figure 6c). Dechlorinator biomass (Figure 6d) dropped from the initial estimated steady-state level of 2.3 mg of VSS, to approximately 1.7 mg of VSS. The mass of the other organism types, including

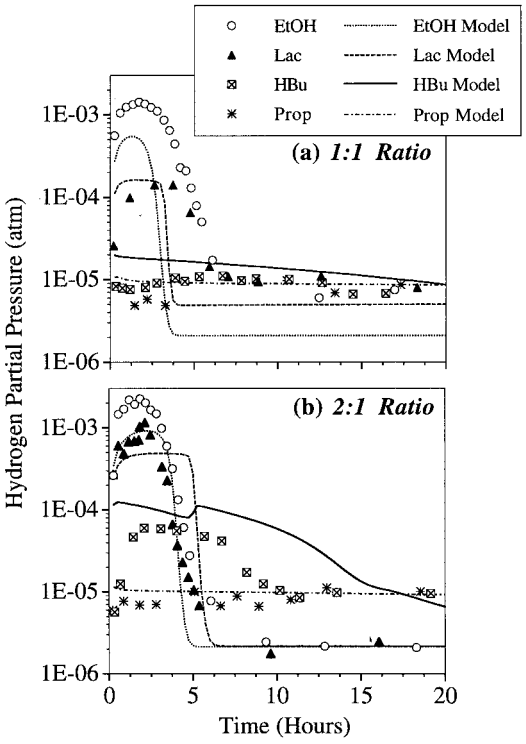

FIGURE 5. Comparison of model predictions with hydrogen production from the degradation of ethanol, lactic acid, butyric acid, and propionic acid at a (a) 1:1 (equiv/equiv) donor to PCE ratio and (b) 2:1 (equiv/equiv) donor to PCE ratio.

hydrogenotrophic methanogens, also decreased. The final biomass content of the simulated culture was 2.3 mg of VSS/100 mL.

Figure 7 shows the same 1:1 ethanol simulation, but *with* FYE amendment. This compares favorably to the experimental results from such a culture (*9*). PCE dechlorination—initially incomplete—eventually became complete to VC and ETH and continued to improve (Figure 7a). Hydrogenotrophic methanogenesis decreased over time (Figure 7b). Traces of propionic acid and, more significantly, butyric acid accumulated in the culture from the FYE input (Figure 7c). Note that dechlorinator biomass did not decrease to the same extent as it did in the simulation where FYE was omitted; however, the loss of hydrogenotrophic methanogen biomass was greater (Figure 7d). The final total biomass content was 2.7 mg of VSS/100 mL, compared to an actual biomass content in the 1:1 ethanol-amended culture of 3.2 mg of VSS/100 mL.

(b) Simulation of Ethanol at a 10:1 Ratio. A 10:1 ethanol to PCE ratio simulation was run to determine whether by simply adding a higher donor to PCE ratio, ethanol (without FYE) *could* support complete dechlorination. The repetitive amendments for this simulation were 220 μmol of ethanol, 11 μmol of PCE, and no FYE. The initial biomass settings were the same as those used for the 1:1 ethanol to PCE simulation. The results are shown in Figure 8. While initially complete, dechlorination eventually failed in the simulated system (Figure 8a). Methanogenesis from H_2 came to predominate as a bioprocess (Figure 8b). The hydrogenotrophic methanogenic population increased 5-fold, and the dechlorinator biomass decreased during the run (Figure 8d). Although butyric acid accumulated through endogenous decay (Figure 8c), the amount contributed did not restore complete dechlorination. The total biomass accumulated by the end of the run was 12 mg of VSS/100 mL. Since actual cultures were not run under these conditions and since FYE is thought to supply some unidentified nutrient, it was not possible to confirm these model results experimentally.

Discussion

A comprehensive biokinetic model employing Michaelis–Menten-type kinetics, H_2 thresholds for dechlorinators and methanogens, and thermodynamic limitations on donor fermentation successfully described experimental data from mixed anaerobic cultures in which methanogens and dechlorinators competed for H_2. While some differences existed between model-predicted and experimental results, the model captured very well the markedly different patterns of H_2 evolution and consumption among four donors evaluated at two levels of donor:PCE (Figure 5). These conditions resulted in H_2 peaks—both in simulated and experimental data—that ranged over nearly 3 orders of magnitude. Whatever degree of satisfaction/dissatisfaction one might take in the observed degree of accord between simulated and experimental data, we must emphasize that it was accomplished using a single set of biokinetic and thermodynamic parameter values for all simulations. In some instances, discrepancies probably resulted from the fact that the biomass levels used as inputs to TIS simulations were based on steady-state analysis predictions of the cultures; much of the collected data were obtained under obviously non-steady-state conditions.

The thermodynamic foundation of our model—the dependence of fermentation upon rate of H_2 removal—has been well-recognized and verified by other investigators (*15*, *26*, *30*, *38*, *39*). While the model may appear to be very complex (and we admit that it is conceptually challenging), our incorporation of these syntrophic, thermodynamic concepts does not introduce difficult issues of parameter estimation. Free-energy values are readily "knowable", and critical-free-energy values estimated by several investigators have yielded remarkably similar values of about −20 kJ/mol (*26*–*31*). Incorporation of threshold concentrations for H_2 use by dechlorinators and methanogens reflects experimentally observed reality; however, precise knowledge of the specific threshold values is not critical—knowing the relative values among competing microbial groups is sufficient, and since these differences also have a thermodynamic basis, there is reason to suggest that these relative differences may have universal application.

The model form we propose could be employed (obviously with modification of parameter values to reflect site-specific conditions, such as temperature) as the biokinetic component of a complete, subsurface fate-and-transport model. Such a comprehensive model would certainly find use in natural-attenuation applications; however, it would be essential in situations where enhanced bioremediation of chloroethenes is contemplated. It is clear from our results that different prospective donors will behave differently, in terms of either exacerbating or minimizing unwanted competition for H_2. Our approach to modeling the biokinetics of reductive dechlorination and its competing processes would allow alternative amendment strategies to be explored in a realistic manner. For example, in a scenario where ethanol were proposed as donor, the resulting increased methanogenic activity in the injection zone would be predicted—along with its long-term consequences to competition for H_2 and deleterious effects on enhanced remediation of the targeted chloroethenes. Such effects are not predictable if one assumes perpetual first-order degradation of chloroethenes—

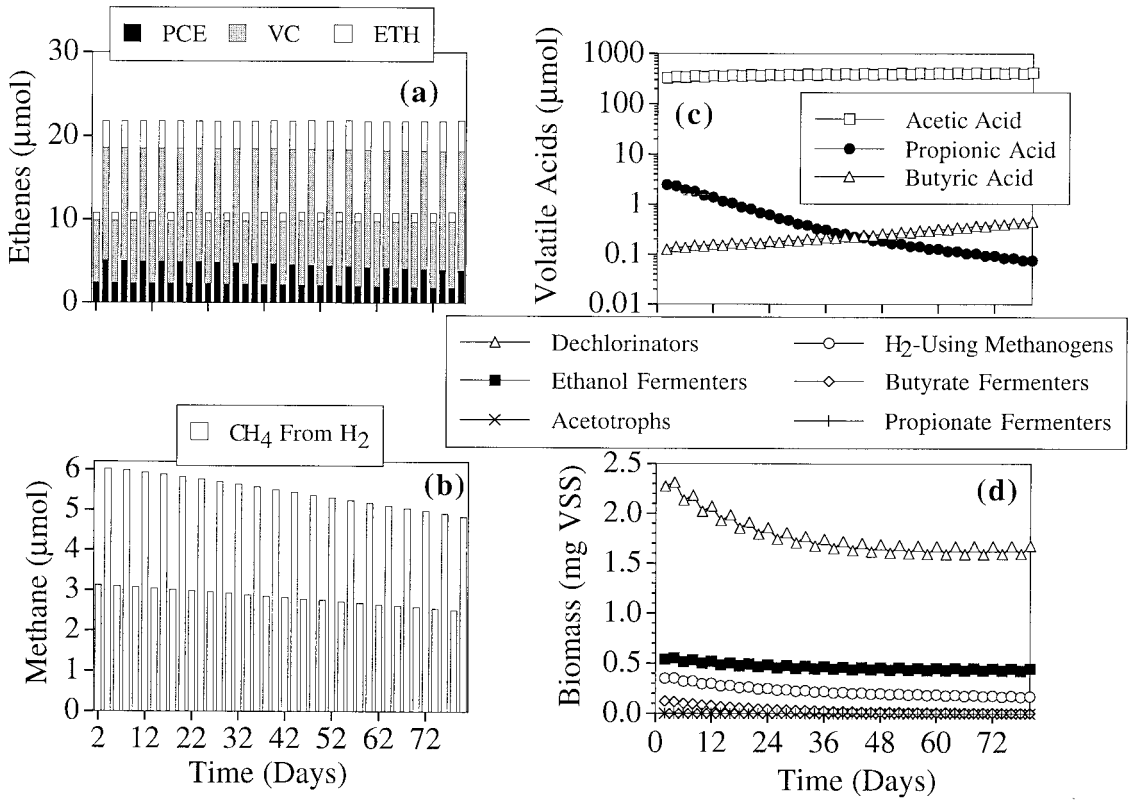

FIGURE 6. Long-term simulation of ethanol-amended culture fed 1:1 (equiv/equiv) donor to PCE ratio without FYE amendment: (a) dechlorination; (b) methane from hydrogen; (c) VFAs; and (d) biomass.

an assumption of unlimited availability and undifferentiated degradation kinetics of the donor(s).

Several other models utilize more descriptive kinetics (*11*−*13*) and one includes both chloroethene and electron-donor degradation kinetics, equations for the conversion of an applied donor to endproducts thought to be used by dechlorinators, and competitive inhibition between PCE and TCE (*14*). However, the key, missing model ingredients are the incorporation of H_2 thresholds for hydrogenotrophs, and the thermodynamic limitation on H_2 "ceiling" for fermentation. For example, it was thermodynamic limitation—and not intrinsic kinetics—that was responsible for lack of H_2-peaking observed with propionate-fed systems (Figure 5).

In a case when the H_2 use rate is rapid and steady—for example, when ample PCE is present—straightforward Michaelis−Menten kinetics might be sufficient to describe donor degradation and H_2 production. It also might be sufficient to describe fermentation of high-H_2-ceiling substrates (e.g., lactate), where H_2 level is a less-important influence on fermentation kinetics. However, low-H_2-ceiling substrates (e.g., propionate) are the very ones recommended to selectively enhance dechlorination while managing competition for H_2 (*9*). Fermentation of such substrates—and their persistence downgradient from point of application—are greatly influenced by H_2 level and hence by rate of H_2 consumption by dechlorinators and their competitors. Thus, one would require the use of a different set of "apparent" fermentation kinetic parameters, depending on the H_2-utilization rate of the system under consideration. But while such system-specific kinetic parameters might prove adequate in some circumstances, it is troublesome that kinetic parameters must be so modified.

Even with such modifications, this "simple" approach has deficiencies that become all-too-apparent when H_2 consumption suddenly slows as PCE is exhausted (leaving only the more slowly degraded VC). In such instances, there is a step change to a lower rate of fermentation that cannot be described via simple Michaelis−Menten kinetics. If one examines our 2:1 propionate-fed system shown in Figure 2, one can observe an apparent break in the rate of propionate fermentation after PCE is depleted, at about 20 h. The depletion of PCE and the subsequently slower rate of H_2 use—now coupled to VC dechlorination—is accompanied by a slight rise in the H_2 level which effectively slows the propionate fermentation rate. The model captures the break in rate along with the other consequences. Straightforward Michaelis−Menten kinetics could not capture these phenomena, illustrating the need for a modeling approach that includes consideration of the thermodynamics of syntrophy. Furthermore, the level of H_2 in a system is critical to determining the proportion of donor equivalents that will go to dechlorination, as opposed to competing methanogenesis, as well as impacting donor fermentation rate. Modeling H_2 dynamics becomes critical to accurate modeling of these complex, mixed-culture dechlorination systems.

The importance and significance of being able to predict the different behaviors of different donors was shown by simulating ethanol-fed systems. Simulation of 1:1 ethanol-amended cultures showed failure of dechlorination when FYE was withheld, while when FYE was added, dechlorination reached completion. The simulated dechlorinator population was more stable when FYE addition was included, since these organisms can out-compete hydrogenotrophic methanogens for low-level H_2. A simulation wherein the ethanol amendment was simply increased to a 10:1 ratio (in the absence of FYE addition) initially showed complete dechlorination of the PCE to VC and ETH; however, after prolonged simulated operation, dechlorination failed because a large hydrogenotrophic methanogen population developed on the high-level H_2 source. The simulation reinforces experimental results demonstrating that the quality of the H_2 donor is very important to consider when planning in situ stimulation of

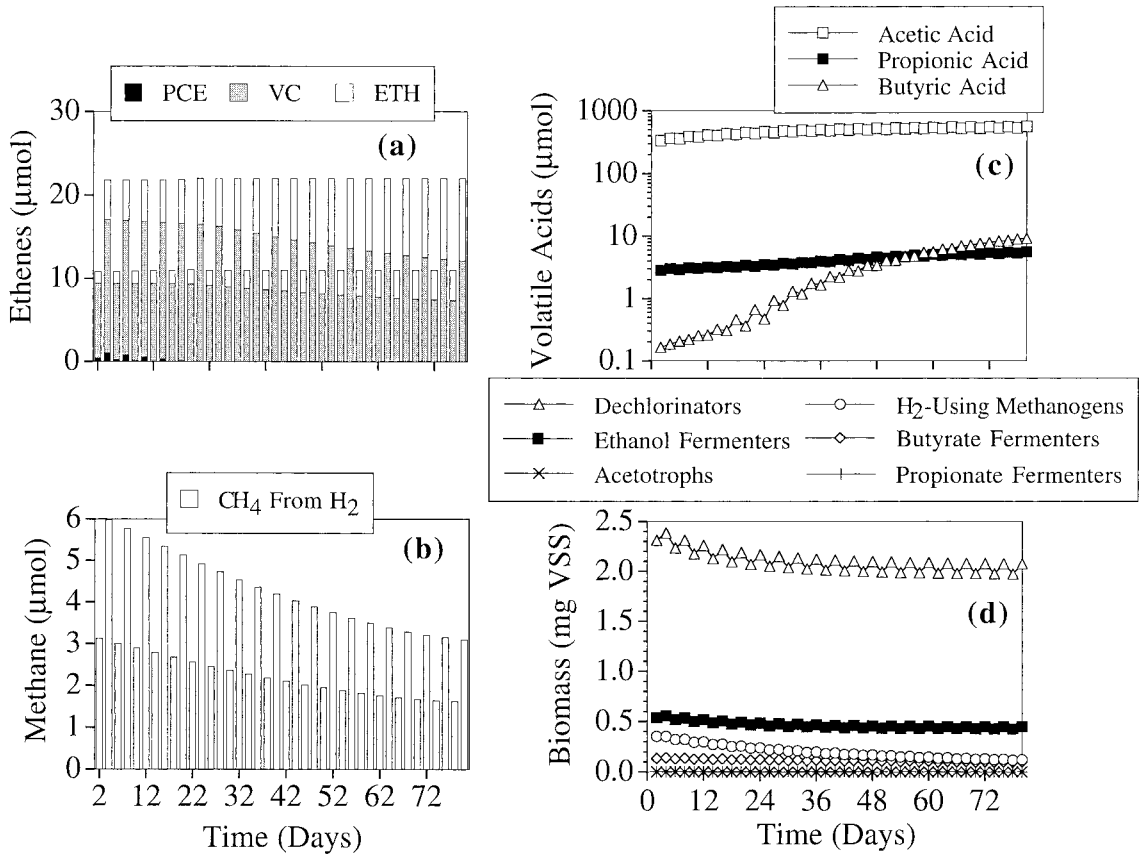

FIGURE 7. Long-term simulation of ethanol-amended culture fed 1:1 (equiv/equiv) donor to PCE ratio with FYE amendment: (a) dechlorination; (b) methane from hydrogen; (c) VFAs; and (d) biomass.

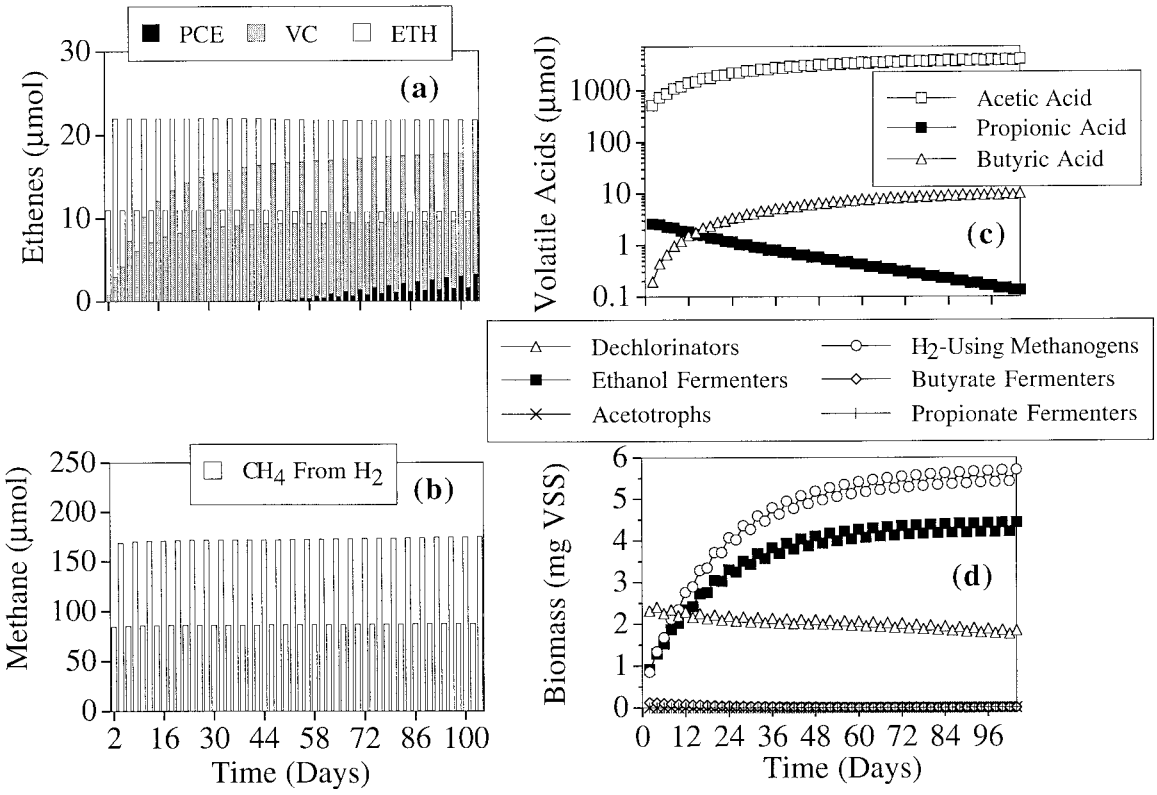

FIGURE 8. Long-term simulation of ethanol-amended culture fed 10:1 (equiv/equiv) donor to PCE ratio without FYE amendment: (a) dechlorination; (b) methane from hydrogen; (c) VFAs; and (d) biomass.

reductive dechlorination or when trying to predict the outcomes at naturally attenuated sites.

The successful simulation of the experimental data collected for the different donors validates the approach used for the model and demonstrates that the model is a useful one for simulating and predicting the behavior of dechlorinating systems amended with or possessing different donors. The biokinetic model could easily be extended to include components for other donors and their accompanying thermodynamic properties or other competing hydrogenotrophs (e.g., sulfate-reducing bacteria) with their intrinsic H_2 thresholds. The model is promising as a useful and more descriptive biokinetic component that could be incorporated into fate-and -transport models used for predicting natural attenuation or enhanced bioremediation. While the kinetic parameters we employed may be specific to our laboratory-culture systems at 35 °C, the model structure, on the other hand, should have more universal applicability, given its sound fundamental basis.

Acknowledgments

This research was supported by the U.S. Air Force Armstrong Laboratory, Environmental Quality Directorate, Tyndall AFB, FL, under Contract F08637-97-M-6001, and through a Selected Professions Fellowship from the American Association of University Women Educational Foundation.

Literature Cited

(1) Scholz-Muramatsu, H.; Neuman, A.; Messmer, M.; Moore, E.; Diekert, G. *Arch. Microbiol.* **1995**, *163*, 48−56.
(2) Holliger, C.; Schraa, G.; Stams, A. J. M.; Zehnder, A. J. B. *Appl. Environ. Microbiol.* **1993**, *59*, 2991−2997.
(3) Holliger, C.; Schumacher, W. *Antonie van Leeuwenhoek* **1994**, *66*, 239−246.
(4) Maymó-Gatell, X.; Chien, Y.; Gossett, J. M.; Zinder, S. H. *Science* **1997**, *276*, 1568−1571.
(5) Lovely, D. R.; Chapelle, F. H.; Woodward, J. C. *Environ. Sci. Technol.* **1994**, *28*, 1205−1210.
(6) Smatlak, C. R.; Gossett, J. M.; Zinder, S. H. *Environ. Sci. Technol.* **1996**, *30*, 2850−2858.
(7) Ballapragada, B. S.; Stensel, H. D.; Puhakka, J. A.; Ferguson, J. F. *Environ. Sci. Technol.* **1997**, *31*, 1728−1734.
(8) DiStefano, T. D.; Gossett, J. M.; Zinder, S. H. *Appl. Environ. Microbiol.* **1991**, *57*, 2287−2292.
(9) Fennell, D. E.; Gossett, J. M.; Zinder, S. H. *Environ. Sci. Technol.* **1997**, *31*, 918−926.
(10) Wiedemeier, T. H.; Swanson, M. A.; Moutoux, D. E.; Gordon, E. K.; Wilson, J. T.; Wilson, B. H.; Kampbell, D. H.; Hansen, J. E.; Haas, P.; Chapelle, F. H. *Technical protocol for evaluating natural attenuation of chlorinated solvents in groundwater*; U.S. Air Force Center for Environmental Excellence: San Antonio, TX, 1996.
(11) Sun, Y.; Petersen, J. N.; Clement, T. P.; Hooker, B. S. *Symposium on Natural Attenuation of Chlorinated Organics in Groundwater*; Dallas, TX, 1996; pp 170; EPA-540/R-96/509.
(12) Rifai, H. S.; Newell, C. J.; Miller, R. N.; Taffinder, S.; Rounsaville, M. In *Intrinsic Bioremediation*; Ward, H., Ed.; Battelle Press: Columbus, OH, 1995; pp 53−59.
(13) de Blanc, P. C.; McKinney, D. C.; Speitel, G. E., Jr.; Sepehrnoori, K.; Delshad, M. In *Non-Aqueous Phase Liquids (NAPLs) in Subsurface Environments: Assessment and Remediation*; Reddi, L. N., Ed.; ASCE: Washington, DC, 1996; pp 478−489.
(14) Tonnaer, H.; Alphenaar, A.; de Wit, H.; Grutters, M.; Spuij, F.; Gerritse, J.; Gottschal, J. C. In *In situ and On-Site Bioremediation: Papers from the Fourth International In Situ and On-Site Bioremediation Symposium*; Alleman, B. C., Leeson, A., Eds.; Battelle Press: Columbus, OH, 1997; Vol. 5, pp 591−596.
(15) Powell, G. E. *J. Chem. Technol. Biotechnol.* **1984**, *34*B, 97−100.
(16) Archer, D. B.; Powell, G. E. *Arch. Microbiol.* **1985**, *141*, 133−137.
(17) Kreikenbohm, R.; Bohl, E. *FEMS Microbiol. Ecol.* **1986**, *38*, 131−140.
(18) Labib, F. Ph.D. Dissertation, University of Washington, 1989.
(19) Labib, F.; Ferguson, J. F.; Benjamin, M. M.; Merlgh, M.; Ricker, N. L. *Environ. Sci. Technol.* **1992**, *26*, 369−376.
(20) Labib, F.; Ferguson, J. F.; Benjamin, M. M.; Merigh, M.; Ricker, N. L. *Environ. Sci. Technol.* **1993**, *27*, 2673−2684.
(21) Hoh, C. Y.; Cord-Ruwisch, R. *Biotechnol. Bioeng.* **1996**, *51*, 597−604.
(22) *Standard Methods for the Examination of Water and Wastewater*, 16th ed.; American Public Health Association, American Water Works Association, Water Pollution Control Federation: New York, 1985.
(23) McCarty, P. L. Presented at the Fifth Rudolf Research Conference, Rutgers, The State University, New Brunswick, NJ, July 1969.
(24) Smatlak, C. R. Master of Science Thesis, Cornell University, 1995.
(25) Fennell, D. E. Ph.D. Dissertation, Cornell University, 1998.
(26) Seitz, H.-J.; Schink, B.; Pfennig, N.; Conrad, R. *Arch. Microbiol.* **1990**, *155*, 82−88.
(27) Schink, B. *Microbiol. Molecul. Biol. Rev.* **1997**, *61*, 262−280.
(28) Dwyer, D. F.; Weeg-Aerssens, E.; Shelton, D. R.; Tiedje, J. M. *Appl. Environ. Microbiol.* **1988**, *54*, 1354−1359.
(29) Schink, B.; Friedrich, M. *FEMS Microbiol. Rev.* **1994**, *15*, 85−94.
(30) Wallrabenstein, C.; Schink, B. *Arch. Microbiol.* **1994**, *162*, 136−142.
(31) Warikoo, V.; McInerney, M. J.; Robinson, J. A.; Sulflita, J. M. *Appl. Environ. Microbiol.* **1996**, *62*, 26−32.
(32) Cord-Ruwisch, R.; Seitz, H.-J.; Conrad, R. *Arch. Microbiol.* **1988**, *149*, 350−357.
(33) Lovely, D. R. *Appl. Environ. Micro.* **1985**, *49*, 1530−1531.
(34) Lovely, D. R.; Goodwin, S. *Geochim. Cosmochim. Acta* **1988**, *52*, 2993−3003.
(35) Chapelle, F. H. *Symposium on Natural Attenuation of Chlorinated Organics in Groundwater*, Dallas, TX, 1996; pp 17−20; EPA-540/R-96/509.
(36) Lovely, D. R.; Ferry, J. G. *Appl. Environ. Micro.* **1985**, *49*, 247−249.
(37) Krzycki, J. A.; Morgan, J. B.; Conrad, R.; Zeikus, J. G. *FEMS Microbiol. Lett.* **1987**, *40*, 193−198.
(38) Ahring, B. K.; Westermann, P. *Appl. Environ. Microbiol.* **1988**, *54*, 2393−2397.
(39) Seitz, H.-J.; Schink, B.; Pfennig, N.; Conrad, R. *Arch. Microbiol.* **1990**, *177*, 89−93.
(40) Tandoi, V.; DiStefano, T. D.; Bowser, P. A.; Gossett, J. M.; Zinder, S. H. *Environ. Sci. Technol.* **1994**, *28*, 973−979.
(41) Young, R. G.; Gossett, J. M. Cornell University, unpublished data, 1997.
(42) Robinson, J. A.; Tiedje, J. M. *Arch. Microbiol.* **1984**, *137*, 26−32.
(43) Giraldo-Gomez, E.; Goodwin, S.; Switzenbaum, M. S. *Biotechnol. Bioeng.* **1992**, *40*, 768−776.
(44) Goodwin, S.; Giraldo-Gomez, E.; Mobarry, B.; Switzenbaum, M. S. *Microbial Ecol.* **1991**, *22*, 161−174.
(45) Ohtsubo, S.; Demizu, K.; Kohno, S.; Miura, I.; Ogawa, T.; Fukuda, H. *Appl. Environ. Micro.* **1992**, *58*, 703−705.
(46) Zehnder, A. J. B.; Huser, B. A.; Brock, T. D.; Wuhrmann, K. *Arch. Microbiol.* **1980**, *124*, 1−11.
(47) Ahring, B. K.; Westermann, P. *Appl. Environ. Microbiol.* **1987**, *53*, 434−439.
(48) Tholozan, J. L.; Touzel, J. P.; Samain, E.; Grivet, J. P.; Prensier, G.; Albagnac, G. *Arch. Microbiol.* **1992**, *157*, 249−257.
(49) Wallrabenstein, C.; Hauschild, E.; Schink, B. *Arch. Microbiol.* **1995**, *164*, 346−352.
(50) Schink, B. *Arch. Microbiol.* **1984**, *137*, 33−41.
(51) Daniels, L.; Sparling, R.; Sprott, G. D. *Biochim. Biophys. Acta.* **1984**, *768*, 113−163.
(52) Weimer, P. J.; Zeikus, J. G. *Arch. Microbiol.* **1978**, *119*, 49−57.

Received for review February 9, 1998. Revised manuscript received May 25, 1998. Accepted May 25, 1998.

ES980136L